Physics of Our Days

EXTREMAL STATES OF MATTER (ULTRAHIGH PRESSURES AND TEMPERATURES)

D. A. KIRZHNITS

P. N. Lebedev Physics Institute, USSR Academy of Sciences

Usp. Fiz. Nauk 104, 489–508 (July, 1971)

1. INTRODUCTION

THE properties of matter in states with unusually high energy concentration (such states and the external conditions corresponding to them will be called extremal) were always of considerable interest in a number of branches of physics and related sciences—astrophysics, geophysics, and some applied disciplines. Investigations of extremal states of matter have become particularly important recently. This is due to the appearance of a number of practical problems (such as the realization of controlled thermonuclear fusion or the production of ultrahard materials), the development of new methods for realizing extremal conditions, the discovery of new extremal states in nature (neutron matter in pulsars), etc.

Foremost among the extremal external conditions are high pressures and high temperatures, to which we confine ourselves in this review. The corresponding region on the "pressure-temperature" diagram can be broken up naturally into a number of individual sections, each corresponding to a special state or to special properties of matter. Such a breakdown can be effected in accordance with various attributes: in accordance with the type of structural units of matter (for example, electron-nuclear and neutronic forms of matter), in accordance with the character of its aggregate state (solid, plasma), in accordance with the role of the interaction and correlations between particles (ideal and nonideal, Boltzmann and degenerate gases), in accordance with the course of the nuclear processes (thermonuclear and pycnonuclear reactions), etc.

In the literature there are sufficiently detailed descriptions of each such state separately. However, the general systematization and classification of the extremal states is given only in part, either separately for high pressures and high temperatures, or only in accordance with some of the attributes listed above (see, for example,[1-7]).

The purpose of the present review is to attempt to fill this gap and to give a general idea of the structure of the region of extremal states as a whole. Principal attention will be paid not to descriptions of individual extremal states, but to their interrelationships and to transitions between them. For the sake of clarity, the results are given in the form of "pressure-temperature" and "density-temperature" diagrams. We point out immediately that transitions between extremal states are in most cases continuous. Therefore the transition lines on the aforementioned diagrams have an arbitrary qualitative meaning and give only order-of-magnitude values.

It is necessary to stipulate from the very outset that the term "matter" is used in this review for a macroscopic extended medium. We omit from consideration therefore such objects as the atomic nucleus, systems produced when high-energy particles collide, etc. even though the conditions inside such objects can be regarded as extremal in a certain sense.

The exposition is planned as follows. Section 2 contains information on natural objects whose matter in an extremal state, and also on the laboratory capabilities of realizing extremal external conditions. In Sec. 3 we indicate the ranges of pressures and temperatures that will be considered in the review. Section 4 is devoted to a classification of the states of the electronic component of matter, and Sec. 5 to the nuclear component. In Sec. 6 we consider different regimes of isothermal nuclear processes. Finally, in Sec. 7 we describe transformations that lead to the occurrence of new forms of matter—neutronic, positronic, photonic, etc. In the main text we attempted to get along without formulas; the relations needed to plot the diagrams and their derivations are contained in appendices.

The following units are used in the review: the pressure P is measured in megabars (1 Mbar $= 10^{12}$ erg/cm^3 $\approx 10^6$ atm), the temperature T in electron volts (1 eV $\approx 10^{-12}$ erg $\approx 10^4$ deg), and the density ρ in g/cm^3. The following notation is used: m is the electron mass, M the nucleon mass, Z the atomic number (or charge of the ion), A the mass number, n the electron concentration, and N the concentration of the nuclei (ions). The Boltzmann constant is assumed equal to unity.

For reasons indicated in Sec. 3, we do not consider the region of relatively low pressures (below 10^2 Mbar) and temperatures (below 10 eV); this region is more accurately defined by curve 1 of Fig. 1 below. The readers interested in this region can refer to the monographs and reviews[1-21].

2. EXTREMAL STATES IN NATURE AND UNDER LABORATORY CONDITIONS

Figure 1 shows several characteristic objects whose matter is under extremal conditions, and also notes the pressure and temperature regions accessible to research under laboratory conditions.

Under natural conditions extremal states are produced principally by gravitational forces. These forces, which have an unscreened long-range character, compress the matter and, as a consequence, heat it (directly or by increasing the probability of the nuclear processes in which energy is released). Therefore typical examples of extremal states should be sought in the interior of the earth, in celestial bodies, and in the universe during its earlier evolution stages.

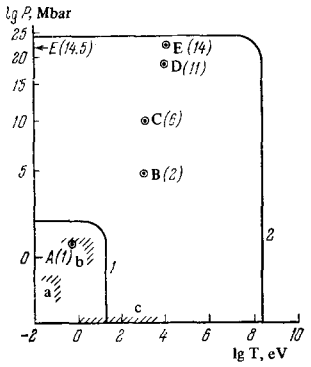

FIG. 1. Extremal states in nature and under laboratory conditions. A) Earth's center, B) sun's center, C) center of white dwarf, D) crust of pulsar, E) mantle of pulsar, E) nuclear matter. The numbers in parentheses are the logarithms of the density (in g/cm^3). Regions a and b correspond to the static and dynamic methods of obtaining high pressures, and region c to methods of obtaining high temperatures. Curves 1 and 2 are the boundaries of the region of extremal states considered in this review.

At the center of the earth (point A on Fig. 1) the pressure reaches about 4 Mbar, the density 10–20 g/cm^3, and the temperature approximately 0.5 eV[17,22]. At the center of the sun (point B) we deal approximately with 10^5 Mbar, 10^2 g/cm^3, and 10^3 eV[23]. Pressures reaching 10^{16} Mbar and a density up to 10^9 g/cm^3 are realized in cooling stars (white dwarfs)[24,25]. The point C corresponds to conditions typical of the core of a white dwarf, namely 10^{10} Mbar, 10^6 g/cm^3, and 10^3 eV. The recently discovered pulsars[26-28] are examples of an object with unprecedented extremal conditions. Deferring the details to the end of Sec. 7 (see also Fig. 9), we point out that typical conditions for the crust of the pulsar are 10^{18} Mbar, 10^{11} g/cm^3, and 10^4 eV (point D), and for the Mantle* the respective values are 10^{22} Mbar, 10^{14} g/cm^3, and 10^4 eV (point E). The density of matter in the atomic nucleus is 3×10^{14} g/cm^3 (point F). We emphasized that data pertaining to the upper part of the diagram are very tentative and give only a general idea of the orders of magnitude.

The extremal states realized under laboratory conditions, in spite of the progress reached in this field, are characterized by much more modest figures.

The static method based on the use of special mechanical devices[8-10], yields pressures on the order of ½ Mbar; this figure will probably reach 1 Mbar in the nearest future. Simultaneously with compression, it is possible to attain heating to a temperature on the order of 0.1 eV (region a in Fig. 1). Dynamic methods are based on the use of powerful explosion shock waves[11,12]. They make it possible to reach pressures of several dozen Mbar. The temperature then reaches 1–10 eV (region B).

The methods that can be used to obtain high temperatures are quite varied, powerful discharge in a plasma, resonant heating with an electromagnetic field, injection of pre-accelerated plasmoids into a plasma, heating with lasers, etc.[21,29,30]. The temperatures reached by now exceed 10^3 eV (region c).

3. BOUNDARIES OF THE REGION OF EXTREMAL STATES

Let us separate the region of pressures and temperatures that will be considered in the present review.

At relatively low pressures and temperatures, matter continues to exhibit the exclusive variety of forms which it possesses in the cold uncompressed state. Accordingly, the characteristics of matter continue to be quite abrupt and nonmonotonic functions of its composition. The classification of the states of matter under this condition is a complicated and cumbersome problem, far beyond the scope of the present brief review.

With increasing pressure or temperature, however, matter acquires a more and more universal structure, and its characteristics become continuously smoother functions of the composition. This clearly pronounced tendency is connected with the fact that, owing to the increase of the internal energy of matter, a definite ordering and "simplification" of its structure becomes possible. The molecules or molecular complexes become destroyed with increasing pressure or temperature, and matter goes over into the purely atomic state. The electron shells of the atoms become realigned, the filling of the levels becoming increasingly regular. Simultaneously, the outer electrons, which determine the chemical individuality of matter, become detached. Finally, if the matter remains in the solid state during the compression and heating, its crystal lattice also becomes ordered. Going through a series of structural transformations, it becomes more and more closely packed and acquires in final analysis a single structure common to all substances (body-centered cubic*).

Such "universalization" of the properties of matter arises when the increment of its energy as a result of compression or heating becomes larger than the characteristic energies of the aforementioned realignments. In order of magnitude, these energies (per particle) do not exceed the energy of the outer electrons of the atom $e^2/a_0 \sim 10$ eV, where $a_0 = \hbar^2/me^2$ is the Bohr radius of the electron; the corresponding energy density is of the order of $e^2/a_0^4 \sim 10^{14}$ erg/cm^3. Therefore the lower boundary of the region of the universal state of matter corresponds to a temperature on the order of 10 eV and to a pressure on the order of 10^2 Mbar (see curve 1 of Fig. 1 and Appendix 1). Only at a sufficiently large distance from this boundary, at larger P or T, is some general description of the properties of matter possible at all. It must be stipulated that the universality we have in mind pertains to the atomic-molecular level; it disappears in those cases when the shell structure of the atomic nucleus becomes important.

The upper boundary of the region considered below is determined by the extent of our knowledge of high-energy physics. We assume that the energy increment due to heating or compression should not exceed about $mc^2 \sim 1$ GeV per particle, i.e., we confine ourselves to a region that is nonrelativistic with respect to the nucleons. We stay in any case below the threshold of production of such hypothetical particles as quarks or intermediate bosons. At higher temperatures or pres-

*We use geophysical terminology in view of the clear outward similarity between the structure of a pulsar and that of the earth.

*This structure is the most favored only at such extremal conditions when the electrom shells of the atom cease to exist.

sures the properties of matter would turn out to be radically dependent on whether such particles actually exist.

The energy increment $\Delta E \sim 1$ GeV assumed by us corresponds to a characteristic length $\hbar c/\Delta E \sim 2 \times 10^{-14}$ cm and to an energy density on the order of 10^{37} erg/cm^3. Therefore the discussed upper boundary is determined by a temperature on the order of 10^9 eV and a pressure on the order of 10^{25} Mbar. The general form of this boundary is given by the curve 2 of Fig. 1 (see Appendix 1). Beyond this limit we are left with the conditions in the earliest stages of the evolution of the universe, in a number of celestial bodies that undergo collapse or catastrophic stages of their evolution, and possibly also in the cores of massive pulsars.

As seen from Fig. 1, the conditions realized in laboratory experiments are on the whole insufficiently extremal for matter to go over into the universal state. Our concepts concerning the properties of matter in the region considered below are therefore based principally on theoretical considerations, which for the time being can be confirmed with the aid of experiments and observations only to a very insignificant degree. Yet the possibilities of a theoretical analysis are strongly limited by the need for taking into account the interactions between particles, and near the upper boundary of the region under consideration we do not have even a reliable theoretical foundation, since there is no consistent theory of strong interactions. For this reason there are still many problems to be solved in the physics of extremal states.

4. STATES OF ELECTRONIC COMPONENT OF MATTER

So long as matter remains in the usual electron-nuclear form (concerning other forms see Sec. 7 below), many of its properties are determined mainly by the electrons—the lightest structural units of matter. The present section is devoted to the classification of the states of the electronic subsystem.

It has already been noted that on going through the boundary of the universal state of matter (curves 1 of Fig. 1 and 2) the outer electrons of its atoms turn out to be completely shared. Any substance that remains solid in such a transition has metallic properties. In the language of band theory, the "metalization" of matter is connected with broadening of the energy bands, as a result of which the electron Fermi level must ultimately fall inside the allowed band. For matter in the transcritical gaseous-liquid state, the crossing of curve 1 leads to the plasma state*. At not very high temperatures, the plasma is strongly nonideal and close to an ordinary liquid from the point of view of the character of ion motion (see Sec. 5).

The remaining electrons of atoms with a value of Z that is not small remain near curve 1 in a bound state.

*We point out that the degree of ionization on curve 1 itself is already quite high [1]. Analogously, metallization of semiconductors having a narrow forbidden band begins much below this curve. To the contrary, such a substance as nickel can apparently first go over into a dielectric state and only at an approximate pressure of a thousand Mbar it is finally transformed into a metal [18,31].

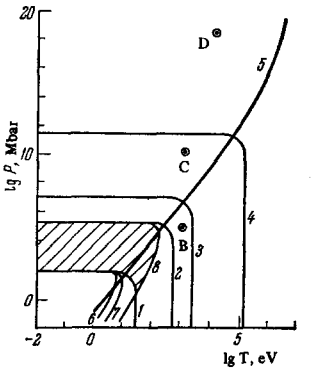

FIG. 2. States of electronic component of matter. 1) Boundary of the region of universality (of the collectivization of the external electrons), 2) of the collectivization of most electrons (Z = 10), 3) of the collectivization of the internal electrons (z = 10), 4) boundary of relativistic region, 5) boundary of degeneracy region, 6) boundary of the region of quasiclassical approach, 7) limit of applicability of the self-consistent-field approximation, 8) boundary of the region of ideality (homogeneity) of electron gas. The shaded region is the one in which the Thomas-Fermi model is applicable.

Their greater part has a binding energy on the order of $G^{4/3}e^2/a_0$ and is localized in a volume on the order of $Z^{-1}a_0^3$ (these estimates result from the Thomas-Fermi model). The boundary where most electrons of the atoms lose their connection with the atom is determined by a temperature of the order of $Z^{4/3} \times 10$ eV and a pressure of the order of $Z^{10/3} \times 10^2$ Mbar (curve 2 of Fig. 2). It still remains to consider the electrons that are closest to the nucleus and are most strongly bound to it, with binding energies on the order of Z^2e^2/a_0 and a localization volume $Z^{-3}a_0^3$. These electrons become collectivized at a temperature of the order of $z^2 \times 10$ eV and a pressure of the order of $Z^5 \times 10^2$ Mbar (curve 3 of Fig. 2). As a result the substance is transformed either into a fully ionized electron-nuclear plasma or into an ideal metal with a lattice made up of "bare" nuclei.

Curves 2 and 3 on Fig. 2 are shown for Z = 10. For arbitrary Z, they can be obtained from curve 1 by assuming that the P and T coordinates are replaced by $Z^{-10/3}P$ and $Z^{-4/3}T$ (curve 2) or $Z^{-5}P$ and $Z^{-2}T$ (curve 3).

At relatively low pressures and temperatures, the motion of the electrons can be regarded as nonrelativistic. The effects of relativity theory become noticeable when the energy increment as a result of the compression or heating reaches a value on the order of mc^2 (the corresponding characteristic length is $\hbar/mc$). This corresponds approximately to 10^{11} Mbar and 10^5 eV (curve 4 of Fig. 2). The formulas on the basis of which curves 1–4 of this figure were plotted are given in Appendix 1.

It is convenient to present the dynamic description of the electronic subsystem in the language of characteristic lengths. Apart from the Bohr radius a_0, there are four such lengths. Foremost are the average distance between electrons $d \sim n^{-1/3}$ (n is the average electron concentration) and the average distance between nuclei $D \sim Z^{1/3}d$. Next comes the de Broglie wavelength of the electron $\lambda = \hbar/p$ (p is its average momentum); at low and high temperatures we have $\lambda \sim n^{-1/3}$ and $\lambda \sim \hbar/(mT)^{1/2}$, respectively. Finally we have the characteristic inhomogeneity length l within which the electron distribution in space changes noticeably. This quantity coincides with the electronic screening radius and is expressed in terms of the already introduced lengths, $l \sim (a_0d^3)^{1/2}/\lambda$; in cold matter $l \sim a_0^{1/2}n^{1/6}$ and in hot matter $l \sim (T/e^2n)^{1/2}$.

The general expressions for the introduced lengths and also the formulas used to plot the pertinent curves are contained in Appendix 2.

At different ratio of the characteristic lengths, we arrive at different states of the electronic subsystem. The inequality $\lambda \ll d$ corresponds to a classical (Boltzmann) electron gas: at $\lambda \sim d$ degeneracy sets in. The curve bounding the region $\lambda \sim d$ is shown in Fig. 2 (curve 5).

The condition $\lambda \ll l$ means that the wavelength of the electron changes little over a length equal to the wavelength. This, as is well known, corresponds to the condition in which the electron motion is quasiclassical. In the opposite limiting case, the behavior of the electrons has an essentially wave-like character. The relation $\lambda \sim l$ corresponds to curve 6 of Fig. 2.

Under the condition $\lambda \ll (a_0 d)^{1/2}$ or, equivalently, $e^2 n^{1/3} \ll p^2/m$, the energy of the Coulomb interaction of a pair of electrons is small compared with their kinetic energy. This, however, still does not lead to smallness of the interaction effect in general. The point is that there is a strong interaction between the electrons and the nuclei. In addition, owing to the long-range character of the Coulomb forces, the electron can interact with a large number of its neighbors. These interactions can be comprehensively described in the language of the average quantities, i.e., within the framework of the Hartree self-consistent-field method. Therefore the inequality in question actually denotes smallness of those effects which cannot be described within the framework of the Hartree approximation. They are called correlation effects and include, besides the exchange effects connected with the Pauli principle, also the correlation effects proper, which describe the deviation of the true interaction from the average one (for details see[4]). A plot of $\lambda \sim (a_0 d)^{1/2}$ is shown in Fig. 2 (curve 7).

At still higher pressures or temperatures, both the just-mentioned electron-nuclear interaction effects and the effects of collective electron-electron interaction become inessential. The electron gas can then be described by the formulas of an ideal gas, and its distribution in space becomes practically homogeneous*. This occurs when the inhomogeneity length l exceeds the largest parameter with the dimension of length; this parameter is the average distance between nuclei D. The $l \sim D$ curve for $Z = 10$ is shown in Fig. 2 (curve 8). For arbitrary values of Z it can be obtained from curve 7 by assuming the axes to represent the quantities $Z^{-10/3}P$ and $Z^{-4/3}T$.

In the region where the electron gas is ideal, the equation of state of matter has a well known form[1], namely $P \sim (\hbar^2/m)n^{5/3}$ (nonrelativism, degeneracy region), $P \sim \hbar c n^{4/3}$ (ultrarelativism, degeneracy region), or $P \sim nT$ (Boltzmann region). At lower temperatures and pressures the equation of state is altered by the effects of the Coulomb interaction, the contribution of the nuclei, etc. For estimates, however, we can continue to use the presented formulas.

*Deferring the details to Appendix 2, we note that in the region of homogeneity an appreciable fraction of the electrons can still be in the bound state (curve 8 lies inside curve 2).

As seen from Fig. 2, curves 6 and 7 lie outside the region considered by us in the review. When describing the electronic subsystem, we can therefore neglect the correlation and quantum effects (the latter reflect the inaccuracy of the quasiclassical approximation), and we can use the Thomas-Fermi model. This pertains to the region shown shaded in the figure; in the remaining part of the region of extremal states of interest the electrons can be regarded in general as an ideal gas. Details concerning the questions discussed in this section can be found in[4,32], and the results of numerical calculations in[33].

Figure 2 shows also several characteristic objects from Fig. 1. We see that the electrons in the central part of the sun form a nonrelativistic ideal gas which which can be regarded as classical, albeit not very far from degeneracy. The hydrogen atoms, which are the predominant components of the matter of the sun, are fully ionized, and the atoms of the heavier elements can still retain a certain fraction of the electrons. In the central parts of white dwarfs, the electron gas is ideal and degenerate. Relativistic effects play a noticeable role. Under these conditions, matter consists of electrons and "bare" nuclei. The same pertains also to matter in the crusts of pulsars, where the electron gas can be regarded as ultrarelativistic.

5. STATES OF NUCLEAR COMPONENT OF MATTER

The states of the nuclear subsystem determine the answers to two important questions, that of the aggregate state of matter and that of the character of the course of the nuclear processes. The first will be considered in this section and the second in the following one.

At high temperatures, when the thermal energy is high compared with the Coulomb energy, matter is a plasma with properties close to those of an ideal gas. With decreasing temperature or with increasing pressure (the latter leads to a decrease of the average distance between nuclei), the role of the Coulomb interaction between the nuclei increases. For this reason, the ordering of the nuclear system, namely the transition of the matter into the crystalline state, becomes energywise favored (on the other side of the line of transition to the crystalline state we deal with a liquid-like plasma[5]). In particular, at zero temperature (and at not too low or not too high pressures) any substance will be in the solid state[34-37].

We confine ourselves to a substance containing nuclei of only one sort, and for simplicity we neglect the change of the effective charge of the ion in the region inside curve 3 of Fig. 2. To make the analysis common to all elements, we begin with natural "nuclear" density and temperature units, AM/A_0^3 and Z^2e^2/A_0, where $A_0 = \hbar^2/AMZ^2e^2$ is the Bohr radius of the nucleus, and we introduce the "reduced" quantities

$$\rho^* = \rho Z^{-6} A^{-4}, \quad T^* = T Z^{-4} A^{-1},$$

the use of which makes the description universal, For the pressure, however, which is determined mainly by the electronic subsystem, such self-similarity will no longer take place. We shall therefore have to deal with a "density-temperature" diagram.

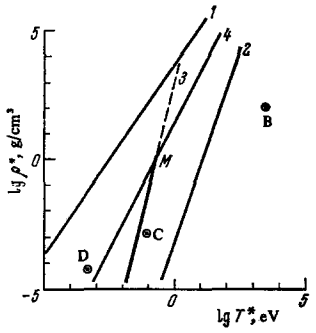

FIG. 3. States of nuclear component of matter. 1) Boundary of the degeneracy region of the nuclei, 2) boundary of the ideality region, 3) melting curve, 4) boundary of the region in which the lattice can be regarded as classical.

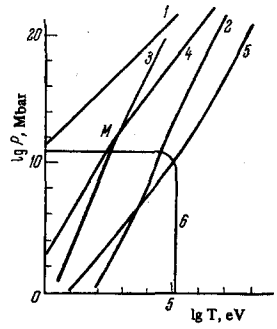

FIG. 4. The same in coordinates P and T for carbon. 5) Boundary of region of electron degeneracy, 6) boundary of region of electron relativism.

In the plasma state, the nuclear subsystem is described by the following characteristic lengths: the average distance between the nuclei $D \sim N^{-1/3}$ ($N = n/Z$ is the average concentration of the nuclei), the de Broglie wavelength of the nucleus $\Lambda \sim \hbar/p$ (p is the average momentum of the nucleus), and the inhomogeneity length $L \sim (A_0 D^3)^{1/2}/\Lambda$, which coincides with the Debye screening radius of the plasma. Just as in the case of the electrons, the line separating the Boltzmann region from the region of degeneracy of the nuclei (see curve 1 on Fig. 3 and Appendix 3) is determined by the condition $D \sim \Lambda$.

The role of the effects of Coulomb interaction in a plasma is determined by the ratio of the lengths D and L. The curve $D \sim L$ is shown in Fig. 3 (curve 2). We point out that it is meaningless to continue the curves of this figure into the region of larger temperatures and pressures, since the light nuclei (hydrogen, helium) "burn out" in this region (see Sec. 6 below), and for heavy nuclei we already found ourselves in a region that is relativistic with respect to nucleons and is excluded from consideration in this review.

The line of interest to us, that of the phase transition into the crystalline state, should lie to the left of curve 2, i.e., in the region where the Coulomb effects play an important role. If both the plasma and the crystal formed from it can be regarded as classical objects, then the equation for the melting curve should not contain Planck's constant. Only one combination of characteristic lengths, being dimensionless, does not contain $\hbar$. This is the ratio D/L. It is therefore obvious that the equation for the melting curve should have the form $D/L = \text{const}$. The value of this constant for strongly compressed matter is close to 10. This corresponds to a Coulomb energy $Z^2e^2N^{1/3}$ which is larger by two orders of magnitude than the thermal energy T^*. We emphasize that the foregoing corresponds exactly to the well known Lindemann criterion, namely the ratio δm of the average amplitude of the oscillations of the nuclei to the average distance between nuclei is constant on the melting curve (see[15,17]). In our case $\delta m \sim 1/4$[38].

The phase-transition line is shown in Fig. 3 (curve 3). Although it lies to the right of curve 1, which determines the boundary of the classical-plasma region, nonetheless the initial premises concerning the applicability of classical statistics are not valid over the entire extent of curve 3. The point is that the character of motion of the nuclei in the crystal is essentially different than that in a plasma. The criterion for the applicability of the Boltzmann statistics will also be different, namely, the amplitude of the zero-point oscillations of the nuclei should be small compared with the total amplitude, which includes also thermal oscillations. This criterion reduces to the obvious condition $\hbar\omega_D \ll T$, where ω_D is the Debye frequency. Under the conditions considered by us $\omega_D \approx 0.45\,\omega_0$, where $\omega_0 = (4\pi NZ^2e^2/AM)^{1/2}$ is the plasma frequency of the nuclei[40]. The plot of $\hbar\omega_D \sim T$ is shown in Fig. 3 (curve 4). The point M where curves 3 and 4 intersect limits the reliable section of the melting point, represented by the thick line. We present also the "pressure-temperature" diagram for $Z = 6$ and $A = 8$ (Fig. 4), which is analogous to the diagram of Fig. 3.

For a rough qualitative description of the course of the melting curve in the quantum region we can use the Lindemann criterion and the known formulas for the quantum oscillator[34]. This is done in Appendix 3, the results of which were used to construct the diagram of Fig. 5. The same figure shows also the usual phase diagram with triple point.

Quantum effects lead to a bending of the melting curve towards higher pressures and lower temperatures. This in turn leads to the appearance of limiting values of the temperature, density, and pressure, above which the crystalline state is impossible. Let us discuss in greater detail the "cold melting" effect, which in principle should take place also at zero temperature (it is precisely this effect which explains the existence of liquid helium at low temperatures and atmospheric pressure; see Appendix 3). Cold melting is due to the

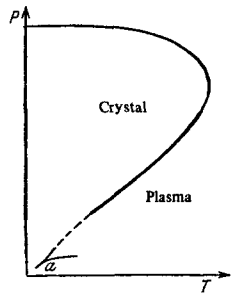

FIG. 5. Approximate form of phase diagram. a) Triple point.

*The change of density in the phase transition, occurring at consent pressure, is quite negligible under the conditions considered here (not more than one-hundredth of one per-cent; see [39]). This allows us to regard the density as a single-valued variable.

zero-point oscillations of the nuclei: the energy of such oscillations $\hbar\omega_D \sim N^{1/2}$ at sufficiently high compressions exceeds the Coulomb binding energy of the lattice, which is proportional to $N^{1/3}$. A reliable description of this phenomenon is hindered by the exceedingly strong dependence of the melting density ρ_m on the Lindemann constant, $\rho_m\delta_m^{12}$, all the more since this constant itself varies to a large degree[41]. The published estimates of ρ_m^* range from 10^3 to 10^8 g/cm^3 [35,40,42-44]. If the very lightest nuclei are excluded, even the relative values of ρ_m and of the nuclear density are not well known. It is therefore not yet clear whether the phenomenon in question is even real.

In concluding this section, let us stop to discuss certain astrophysical application. Figure 3 shows the points corresponding to the conditions at the center of the sun (hydrogen), at the center of a typical white dwarf (carbon), and in the crust of a pulsar (iron). It is seen from the figure that solar matter is in the plasma state, that of the white dwarf in a state close to crystallization[34], and that of the pulsar crust in a solid state[45]. The foregoing pertains, of course, only to the typical conditions assumed by us. There are no grounds for doubting, say, the existence of cold solid white dwarfs.

There is an interesting explanation for the existence of linear sequences of white diagrams on the "luminosity–temperature" diagram[39]. In accordance with this explanation, each line of the diagram corresponds to crystallization of the matter in a white dwarf with definite chemical composition. Let us recall two important properties of the crystallization process: a) the pressure and temperature at which the crystallization takes place are connected by a rigorous relation—the equation of the melting curve; b) owing to the release of the latent heat, the temperature and the pressure remain constant during the time of crystallization. It follows from property (a) that the connection between the luminosity and the surface temperature is also unique, leading precisely to a linear sequence on the diagram. The latent heat released in the crystallization of the matter of a white dwarf is relatively large[34], and is estimated in[39] to amount to T per nucleus. Therefore the crystallization-time interval during which the observed white-dwarf characteristics do not change is also relatively long. For this reason, white dwarfs are most probably observed during the course of their cooling just during the time of their crystallization. The theoretical relations obtain in[39] between the luminosity and the surface temperature agree with observations if reasonable assumptions are made concerning the composition of white dwarfs.

The hard crust of pulsars explain the sharp changes in their angular velocity. As the rotation slows down, shear stresses accumulate in the crust, and from time to time the crust experiences breaks ("starquakes") leading to a change in the pulsar's angular momentum. On the basis of this picture and of the angular-velocity relaxation time, it became possible to show sufficiently convincingly that neutron (proton) matter in the mantle of a pulsar is in the superfluid (superconducting) state[27,28,47,48] (see Ginzburg's review[47] concerning the problem of superconductivity and superfluidity in the universe).

The density in the pulsar's solid crust can be so high that the lattice binding energy, $1.45\ Z^2e^2N^{1/3}$ (per nucleus) for a body-centered-cubic lattice[40], can turn out to be of the order of hundreds of Megaelectron volts. Under these conditions one can expect the lattice to exert a strong influence on the nuclear properties of matter. One can assume, for example, that the fragmentation of the nuclei, which leads to fragmentation of the charge (fission, α decay), may turn out to be inconvenient. In fact, it would mean a transition to a state closer to that of a homogeneous plasma, and would be accompanied by a loss in the lattice binding energy. Thus, for fission into two equal fragments, Z in the preceding formula should be replaced by Z/2, N by 2N, and a factor 2 must be introduced (owing to the increase in the total number of nuclei); as a result, the binding energy decreases in absolute magnitude by a factor $2^{2/3}$. For this reason, superheavy nuclei, for which fragmentation is the main source of instability, might turn out to be stable under conditions of the pulsar's crust. In general, the effects of the crystal lattice lead to a decrease of the Coulomb energy of the nucleus and to an enlargement of the nuclei in the pulsar's crust, increasing the equilibrium values of their mass number and charge by at least 1.5 times[62].

6. EXOTHERMAL NUCLEAR PROCESSES

When the temperature or pressure become large enough, exothermal nuclear transformations (with release of energy) come into play in substances on a noticeable scale. The importance of these processes, let alone thermonuclear fusion under terrestrial conditions, lies in the fact that they are the main source of energy in stars (including the sun), comprise an important factor in the evolution of celestial bodies, and, finally, account for the chemical composition of the substance. Characteristic examples of exothermal reactions are the transformations $4p \rightarrow He^4$ and $3He^4 \rightarrow C^{12}$; the former is realized in accordance with the scheme of the carbon or hydrogen cycle.

Although the reactions in question are accompanied by release of energy, in order for them to occur at a noticeable rate it is necessary that the external conditions be extremal to a sufficient degree. This is necessary to overcome the Coulomb barrier that prevents the reacting nuclei from coming together. The penetrability of the barrier increases because the relative energy of the reagents increases when the substance is heated, or because the barrier itself becomes distorted (narrower) when the substance is compressed. These two nuclear-reaction regimes, called thermonuclear and pycnonuclear, respectively, correspond also to different kinetic mechanisms of the reaction. The rate of a thermonuclear reaction in a plasma is determined, besides the barrier-penetration factor, by the number of partners encountered by one nucleus per unit time as it moves inside the substance. The rate of a pycnonuclear reaction in condensed matter is determined by the number of approaches of the reacting partners, which oscillate about neighboring equilibrium positions, per unit time, i.e., by the frequency of such oscillations. The present section is devoted to a detailed classification of the regimes of nuclear reac-

tions at different temperatures and pressures (see [44,49]).

We confine ourselves for simplicity to a substance consisting of nuclei of one sort, which react with one another.* At relatively high temperatures and low densities, when the plasma differs little from an ideal gas, the barrier-penetration factor almost coincides with the corresponding expression for a pair of isolated nuclei:

$$\exp(-\tau^{1/3}), \quad \tau = \frac{27\pi^2}{4}\frac{Z^2e^2}{A_0T} \sim 1/T^*$$

(cf., e.g.,[50]). Assuming $\tau \gg 1$ (otherwise the substance will burn up too rapidly), the effective energy of the reacting nuclei (the energy of the Gamow peak) lies on the tail of the Maxwellian distribution, $T_{eff} \sim \tau T \gg T$. Owing to the smallness of the average distance between nuclei compared with the Debye radius, the influence of the remaining substance reduces to a small correction to the argument of the exponential; this correction reflects the screening of the Coulomb interaction by the particles that do not participate in the reaction. This is the so-called thermonuclear regime with weak screening. The corresponding region lies to the right of curve 1 on Fig. 6, which coincides with curve 2 of Fig. 3 and corresponds to the condition $D \sim L$.

On going through this boundary, the effects of the Coulomb interaction in the plasma become considerable, and we enter the region of liquid-like plasma, and after crossing curve 3 in Fig. 3 we enter the solid region. From our point of view, however, the difference between these states is inessential, since only the short-range order is of importance for nuclear reactions. The transition of a substance into the condensed state affects strongly the form of the interaction potential between the nuclei, but the nuclei themselves can be regarded as free in a certain sense, even far beyond the boundary of the region in question. The point is that, as already indicated, the effective energy T_{eff} of the colliding nuclei greatly exceeds the real temperature of the system. Actually, therefore, the Coulomb effects become significant from the point of view of the kinetics of the reaction when D becomes of the order of the effective Debye radius, which is obtained from the usual expression by replacing T with T_{eff}. This indeed determines the left-hand boundary of the region in question (see curve 2 of Fig. 2 and Appendix 3); this curve coincides with curve 4 of Fig. 3. The discussed regime is called thermonuclear with strong screening. The penetration coefficient for this regime is strongly altered by the screening effects; an expression for it is given in[49].

At still lower temperatures, the reacting nuclei can also be regarded as "frozen." A decisive role is assumed here by the oscillations of the nuclei about the equilibrium positions. So long as T_{eff} is large compared with $\hbar\omega_D$ (see Sec. 5), these oscillations have mainly a thermal character. This is the pycnonuclear regime with hot nuclei. The left-hand boundary of the region under consideration is determined by the condition $\hbar\omega_D \sim T_{eff}$ (see curve 3 and Appendix 3).

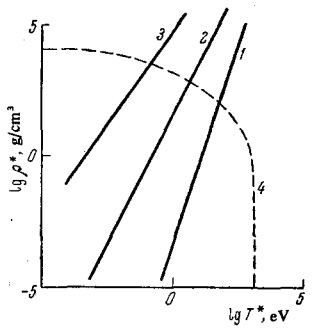

FIG. 6. Regimes of exothermal nuclear reactions. 1) Boundary between thermonuclear reactions with strong and weak screening, 2) boundary between thermonuclear regime with strong screening and the pycnometric regime with hot nuclei, 3) boundary of pycnonuclear regime proper, 4) approximate form of the "threshold" for the hydrogen reaction.

Finally, to the left of this curve we enter in the pycnonuclear regime proper[52,53,44,49], where the reaction proceeds via zero-point vibrations of the nuclei. At sufficiently high compressions, the reaction can occur also at zero temperature, since the Coulomb barrier narrows down to a width on the order of $D \sim N^{-1/3}$. The corresponding penetration factor is given by

$$\exp(-\chi), \quad \chi \simeq 2{,}8/(A_0N^{1/3})^{1/2} \sim \rho^{*-1/6},$$

where, as before, we should assume that $\chi \gg 1$.

Although the reactions in question have no threshold in the exact sense of this word, a noticeable yield of the reaction occurs only at high temperatures or pressures. For the hydrogen reaction this occurs at $T \sim 10^2$–10^3 eV or $\rho \sim 10^4$–10^5 g/cm^3, and for the helium reaction the temperature rises to 10^4 eV. Under simultaneous heating and compression, the corresponding boundary can be found from the cumbersome expressions given in[49] for the penetration factors at all the regimes listed above. We confine ourselves to presenting a purely qualitative curve for the hydrogen reaction (curve 4 of Fig. 6).

We point out by way of an example that nuclear reactions in the interior of the sun and similar stars are thermonuclear reactions with weak screening; this is seen directly from the diagram of Fig. 3.

In concluding this section, let us stop briefly on the reactions $d + d \rightarrow T + p$ (or $\rightarrow He^3 + n$) and $d + T \rightarrow He^3 + n$, which are important from the point of view of "terrestrial" applications. These reactions, unlike the hydrogen reaction considered above, proceed via strong interaction and their purely nuclear cross section is therefore larger by twenty orders of magnitude than the cross section of the hydrogen reaction, which proceeds via weak interaction. However, the "threshold" temperature and the "threshold" density for these reactions are relatively close (in a logarithmic sense) to those indicated in Fig. 6. This is due to the strong dependence of the penetrability factor on T^* and ρ^*. We note that the muonic catalysis once proposed for these reactions by Ya. B. Zel'dovich and A. D. Sakharov can be regarded in a way as a method of "compressing" matter; inasmuch as the radius of the mesic atom is approximately 1/200th of the radius of the ordinary atom, we are dealing here with an increase of the effective density by almost seven orders of magnitude.

*In the general case, it is necessary to replace in the formulas that follow Z^2 by Z_1Z_2 and A by $2A_1A_2/(A_1 + A_2)$, where Z_1, A_1 and Z_2, A_2 are parameters of the reacting nuclei. Reactions between impurity nuclei are discussed in [34,51,49].

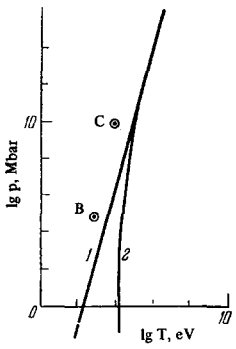

FIG. 7. Photon and positron components of matter: 1) pressure of photonic component, 2) pressure of positronic component.

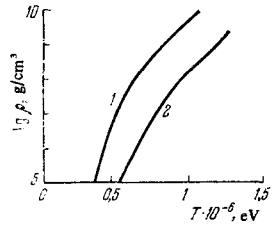

FIG. 8. "Iron–helium–nucleons" thermal dissociation: 1) curve of half-way dissociation of iron, 2–of helium.

7. NEW FORMS OF MATTER

The end result of the processes considered in the preceding section was only a regrouping of the nucleon, leading to a transformation of some nuclei into others. There was no change in the structural composition of the matter at the elementary particle level, and no new forms of matter appeared.* Yet transformations of this type are inevitable at high temperatures and pressures, and play an important role in astrophysics.

We begin with the simplest process, viz., the appearance, at high temperatures, of equilibrium thermal radiation as a separate component of matter making a noticeable contribution to its energy, pressure, etc. Using for the radiation pressure the well known formula $P \sim T^4/\hbar^3c^3$ (see curve 1 of Fig. 7), we readily see that near this curve the photon component of the matter makes a large and even decisive contribution to the pressure.

A very similar picture could be obtained also for the neutrino component of matter. The neutrinos, however, go off from the celestial bodies and can play a role as a separate component of matter only during the earlier stages of the evolution of the universe (see[2]).

Let us proceed to the production of electron-positron pairs and to the appearance of the positron component of matter. This process is endothermal (with a corresponding threshold $2mc^2 \approx 1$ MeV). As seen from the results of Appendix 4, at $T \gg mc^2$ the expression for the positron pressure is practically the same as for radiation, and at $T < 2mc^2$ an exponential threshold factor $\exp(-2mc^2/T)$ appears. The boundary of the region where the positron pressure is substantial is given by curve 2 of Fig. 7. We do not show in the figure the corresponding curves for the production of muon, baryon, and other pairs, the thresholds for which are higher.

The foregoing processes are characterized by the fact that their onset requires thermal excitation of the system. At low temperatures, accordingly, these processes have a negligibly small intensity. They include also thermal dissociation of nuclei, particularly of the nuclei of the stablest isotope F^{56}_{26}. This reaction reduces to the transformations $Fe \rightarrow 13\,He^4 + 4n$ and $He^4 \rightarrow 2p + 2n$, and leads to the appearance of the neutron component of matter. Figure 8 shows a diagram borrowed from[54] (see also[2]). Curve 1 corresponds to half-way dissociation of iron, and curve 2 to helium.

The most important type of transformation occurring in cold matter is its neutronization, i.e., the capture of an electron by the nucleus and conversion of the intranuclear proton into a neutron. The scheme of this reaction is $(A, Z) + e^- \rightarrow (A, Z-1)$. Since the initial nucleus is assumed to be stable, and the resultant neutron-excess nucleus has a higher energy, the neutronization process is endothermal and has a threshold $\Delta Mc^2 = (M^A_{Z-1} - M^A_Z)c^2$. The energy needed to overcome the threshold is drawn in cold matter* from a gravitational source, namely, the gravitation forces compress the star, increase the Fermi energy of the electrons, and accelerate them to the required energy. At high temperatures the neutronization is due to the increase of the thermal energy of the electrons and is connected with the usual chemical-equilibrium mechanism. The neutronization of matter is the subject of a rather extensive literature (cf. e.g.,[1-3,55-59]). However, many pertinent problems still await their quantitative solution, owing to the imperfection of the existing methods for describing multinucleon systems, and especially those containing even heavier particles. We therefore confine ourselves below to several remarks and to a small number of quantitative estimates. The latter, with a few exceptions, are quite approximate.

The neutronization threshold is given by the formula $\rho \sim (Mc^3/\hbar^3)[\Delta M)^2 - m^2]^{3/2}$. The corresponding pressure at $\Delta M \gg m$ is $P \sim c^5(\Delta M)^4/\hbar^2$ (see Appendix 4). We indicate by way of an example that the threshold density and pressure amount to 4×10^{10} g/cm^3 and 6×10^{16} Mbar for the transition $C^{12}_6 \rightarrow B^{12}_5$ and 2×10^9 g/cm^3 and 8×10^{14} Mbar for $Si^{28}_{14} \rightarrow Al^{28}_{13}$.

All pressures above threshold, the nucleus becomes "overloaded" with neutrons. Up to about 10^{11} g/cm^3 and about 10^{18} Mbar these nuclei retain their mass numbers and only their charges decrease. This is due to the fact that the instability of such nuclei outside the substance would be manifest by their β decay. In the substance, however, such a decay is impossible because of the high Fermi boundary of the electrons. At higher densities and pressures the disintegration of the nuclei, which relieves them of the excess neutrons, becomes more convenient. This gives rise to an autonomous neutron component of matter. At still higher densities (presumably near 5×10^{13} g/cm^3) the nuclei disintegrate completely and the matter is transformed

*We disregard to neutrinos and positrons produced in the hydrogen reactions, since they either escape from the substance or are annihilated. In no case do they lead to a new form of matter.

*The term "cold" is quite arbitrary and refers to temperatures that are low compared with ΔMc^2.

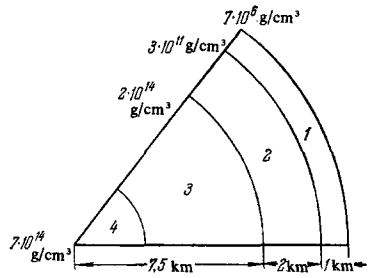

FIG. 9. Model of internal structure of pulsar of medium mass: 1) outer crust (nuclei + electrons), 2) inner crust (nuclei + electrons + neutrons), 3) mantle (neutrons + protons + electrons), 4) core of pulsar (the same + hyperons + mesons).

into a mixture of neutrons, protons, and electrons, with the density of the charged particles smaller by about two orders of magnitude than the neutron density[56,57]. Further increase of the density is accompanied by the appearance of new elementary particles in the substance, which are unstable under ordinary conditions. These are predominantly muons (production threshold about 10^{14} g/cm^3), the decay of which is hindered by the high Fermi boundary of the electrons, followed by hyperons, resonances, etc. (thresholds in the region 10^{14}–10^{15} g/cm^3)[57-59].

The existence in nature of neutron matter was predicted already about forty years ago. It was indicated then that this substance should be sought in the interiors of special (neutron) stars. Such stars were discovered quite recently and were identified with short-period variable sources of radiation, namely pulsars. Figure 1 shows the model of a medium-mass pulsar. This model used presently by astrophysicists[28]. The outer shell, the crust, consists of neutron-excess nuclei and in part of free neutrons. The intermediate layer, the mantle, is a neutron-proton-electron liquid. The central part, the core, contains hyperons, resonances, etc.

* * *

We had to consider in this review a wide region of extremal conditions up to pressures exceeding atmospheric by 30 orders of magnitude and temperatures higher than that of the human body by 10 orders. Such a difference in scales, of course, staggers the imagination. It must be recalled, however, that "...in nature this phenomenon is perfectly natural and commonplace. The domains of some rulers in Germany and Italy, which can be circled in about a half hour, when compared with the empires of Turkey, Muscovy, or China, give only a faint idea of the remarkable contrasts that are hidden in all of nature."[60].

The author is indebted to L. V. Al'tshuler, V. L. Ginzburg, Ya. B. Zel'dovich, S. M. Stishov, and E. L. Feĭnberg for valuable remarks.

APPENDICES

1. LINES OF GIVEN ENERGY INCREMENT

A given energy increment ΔE resulting from heating or compression, corresponds to the condition $\mathscr{E}/n \sim \Delta E$, where $\mathscr{E}$ is the electron energy density and n the electron concentration. It is assumed that ΔE is larger than or of the order of the electron energy in cold uncompressed state. Using the ideal-gas model for estimates, we have

$$\mathscr{E} = 2\int d^3p n_p \varepsilon(p), \quad n = 2\int d^3p n_p,$$

where $d^3p = dp/(2\pi\hbar)^3$, $n_p = [\exp\{(\epsilon(p) - \mu)/T\} + 1]^{-1}$, $\epsilon(p)$ is the electron energy, and μ is the chemical potential. The result will be expressed in terms of Fermi-Dirac functions[61]

$$I_n(\eta) = \int_0^\infty \frac{dx x^n}{\exp(x-\eta)+1},$$

where $\eta = \mu/T$. When $\eta < -4$ and $\eta > 20$ we can use the asymptotic expressions $I_n(\eta) \sim \Gamma(n+1)e^\eta$ and $I_n(\eta) \sim \eta^{n+1}/n+1$, respectively.

In the nonrelativistic case $\epsilon(p) = p^2/2m$ and $P = 2\mathscr{E}/3$, and we obtain a parametric representation of the line of given energy increment in the coordinates P and T or n and T:

$$TI_{3/2}(\eta)/I_{1/2}(\eta) \sim \Delta E, \quad P = \frac{T(2mT)^{3/2}}{3\pi^2\hbar^3} I_{3/2}(\eta), \quad n = \frac{(2mT)^{3/2}}{2\pi^2\hbar^3} I_{1/2}(\eta).$$

In the asymptotic regions we have respectively $T \sim \Delta E$ and $p \sim m^{3/2}\Delta E^{5/2}/\hbar^3$. Curves 1 of Figs. 1 and 2 correspond to $\Delta E \sim e^2/a_0$, curve 2 of Fig. 2 to $\Delta E \sim e^2 Z^{4/3}/a_0$, curve 3 of Fig. 2 to $\Delta E \sim e^2 Z^2/a^0$, and curve 4 of Fig. 2 to $\Delta E \sim mc^2$.

In the ultrarelativistic case $\epsilon(p) = cp$, $P = \mathscr{E}/3$, and

$$TI_3(\eta)/I_2(\eta) \sim \Delta E, \quad P = \frac{T^4}{3\pi^2\hbar^3c^3} I_3(\eta), \quad n = \frac{T^3}{\pi^2\hbar^3c^3} I_2(\eta).$$

In the asymptotic regions $T \sim \Delta E$, $P \sim (\Delta E)^4/\hbar^3c^3$ and $n \sim (\Delta E/\hbar c)^3$. Curve 2 of Fig. 1 is plotted in accordance with these formulas.

2. CHARACTERISTIC LENGTHS OF ELECTRONIC SUBSYSTEM

Using the results of Appendix 1, we can express in explicit form the characteristic lengths introduced in Sec. 4. In the nonrelativistic case the average distance between particles is

$$d \sim \frac{\hbar}{\sqrt{mT}} (I_{1/2}(\eta))^{-1/3},$$

the average de Broglie wavelength is

$$\lambda \sim \frac{\hbar}{\sqrt{mT}} (I_{1/2}(\eta)/I_{3/2}(\eta))^{1/2},$$

and the inhomogeneity length is

$$l \sim \left(\frac{a_0\hbar}{\sqrt{mT}} I_{3/2}(\eta)/I_{1/2}^2(\eta)\right)^{1/2}.$$

The first two expressions are obtained directly, and to derive the third it is necessary to use the Thomas-Fermi equation for the self-consistent potential Φ:

$$\Delta\Phi \sim en \sim \frac{e(mT)^{3/2}}{\hbar^3} I_{1/2}\left(\eta - \frac{e\Phi}{kT}\right).$$

Hence

$$\Delta\Phi \sim \frac{e^2(mT)^{3/2}}{\hbar^3 T} I'_{1/2}(\eta)\Phi \div \ldots, \quad \frac{1}{l^2} \sim \frac{\sqrt{mT}}{\hbar a_0} I'_{1/2}(\eta).$$

In addition, it is easily seen that in the entire range of variation of η the quantity $I'_{1/2}I_{3/2}/I^2_{1/2}$ is of the order

of unity. A direct verification shows that the relation $l^2 \sim a_0 d^3/\lambda^2$ holds (with logarithmic accuracy) at all values of η. In the nonrelativistic case we have $d \sim (\hbar c/T) I_2(\eta)^{-1/3}$, $\lambda \sim (\hbar c/T) I_2(\eta)/I_3(\eta)$.

The relation $\lambda \sim d$ is valid in the region bounded by the curves

$$P \sim m^{3/2}T^{5/2}/\hbar^3, \quad \rho \sim M(mT)^{3/2}/\hbar^3$$

(nonrelativistic case) and $P \sim T^4/\hbar^3c^3$, $\rho \sim M(T/\hbar c)^3$ (ultrarelativistic case). Curve 5 of Fig. 2 is constructed from these formulas.

The relation $\lambda \sim l$ yields $TI^4_{3/2}(\eta)/I^6_{1/2}(\eta) \sim e^2/a_0$. In the degeneracy region $P \sim e^2/a_0^4$, and in the Boltzmann region $P \sim T^3e^4a_0$ (see Fig. 2, curve 6).

Curve 7 of Fig. 2 corresponds to the relation $\lambda \sim \sqrt{a_0 d}$ or

$$TI^2_{3/2}(\eta) \cdot I^{5/3}_{1/2}(\eta) \sim e^2/a_0.$$

In the degeneracy region $P \sim e^2/a_0^4$, and in the Boltzmann region $P \sim T^4/e^6$. The same expressions with e^2/a_0 replaced by $Z^{4/3}e^2/a_0$ correspond to curve 8 of Fig. 2.

Let us make a few remarks concerning the last curve. The statement made in the text that D is the largest of all characteristic lengths (with the exception of l) follows directly from the relations $D \gg d$ at $Z \gg 1$, $d \gtrsim \lambda$, and $d \ll a_0$. We can verify directly that above curve 8 the energy of the electron-nuclear interaction is small compared with the kinetic energy, namely, the condition $l \gg D$ is a direct consequence of the inequality $Ze^2/D \ll p^2/m$. We can estimate analogously also the collective electron-electron interaction.

In the Boltzmann region, curve 8 lies inside curve 2. This means that the electron gas becomes ideal under conditions when a noticeable fraction of the electrons is still in the bound state. Here, of course, there is no contradiction, since we are referring to the ideality of the gas in the mean. The Coulomb energy (per nucleus) of the bound electrons, which is of the order of $nZe^2x_0^2$ ($x_0 \sim Ze^2/T$ is the radius of the "hot" ion), is a fraction on the order of $(D/l)^6$ of the kinetic energy ZT of the electrons. This fraction decreases rapidly on moving away from curve 8 towards higher pressure or temperature.

The last remark concerns the estimate given above for l. This quantity has the meaning of the inhomogeneity length in the distribution of the electrons around each of the nuclei. Accordingly, when considering the equation for the potential Φ, we have left out from its right-hand side the charge density of the nuclei, which is assumed to be independent of Φ. Such a consideration, in any case, is valid so long as $l \lesssim D$. This justifies the equations obtained above, which correspond to curves 6–8 of Fig. 2. The usual Debye screening mechanism comes into play when D becomes smaller than the Debye radius for the plasma, $L \sim l/\sqrt{Z}$ (cf. Appendix 3 below). This corresponds to pressures or temperatures high enough for the electron gas to be regarded as ideal.

3. CHARACTERISTICS OF NUCLEAR SUBSYSTEM

In describing the nuclear system we can confine ourselves to the nonrelativistic relations. In the Boltzmann region relative to the nuclei we have $p \sim (AMT)^{1/2}$. Therefore Λ becomes of the order of D when

$$\rho^* \sim M^{5/2}T^{*3/2}/\hbar^3$$

(curve 1 of Fig. 3).

In the Boltzmann region the length L is of the order of $(T/Z^2e^2N)^{1/2}$. The relation $L \sim D$ gives an expression for curve 2 of Fig. 3

$$\rho^* \sim MT^{*3}/e^6.$$

The point of intersection of curves 1 and 2 corresponds to $T \sim 10^5Z^4A$ eV. This temperature is higher than Mc^2 even for carbon.

The equation for the melting point in the classical region (curve 3) corresponds to $D/L \sim 10$ or

$$\rho^* \cong 10^6 MT^{*3}/e^6.$$

The limit of classical motion of the nuclei is determined by the relation $T \sim \hbar\omega_D$ or

$$\rho^* \sim \frac{M^2}{e^2\hbar^2} T^{*2}$$

(see curve 4 of Fig. 3). The point of intersection of the last two curves corresponds to $T \sim 10^{-6}e^2/A_0$.

Figure 4 is Fig. 3 replotted in the coordinates P and T for the values $Z = 6$ and $A = 12$. Its plotting calls for knowledge of the equation of state of the substance, which is determined mainly by the electronic component. This equation is given by the set of expressions for $P(\eta)$ and $n(\eta)$ (see Appendix 1). In the Boltzmann region relative to the electrons we have $P \sim nT$, and in the degeneracy region $P \sim \hbar^2n^{5/3}/m$ (nonrelativistic case) and $P \sim \hbar cn^{4/3}$ (ultrarelativistic case).

The connection between the Lindemann parameter δ_m and the melting temperature T_m of a quantum crystal is given by the formula

$$\delta_m^2 = \frac{3}{2}\frac{\hbar}{AM}\left(\frac{4\pi N}{3}\right)^{2/3}\left\langle \frac{1}{\omega} \operatorname{cth}\frac{\hbar\omega}{2T_m}\right\rangle,$$

where the averaging is over the phonon spectrum. Changing over to the Einstein model with one frequency, we choose the latter from the condition $1/\omega^2 = \langle 1/\omega^2\rangle \cong 12/\omega_0^2$ [38]. Then putting $\delta_m = \text{const}$, we find

$$T^* \cong \frac{eh}{M}\rho^{*1/2}/\ln\frac{1+y}{1-y}, \quad y = 3{,}7\frac{\hbar}{M^{2/3}e}\frac{\rho^{*1/6}}{\delta_m^2}.$$

The maximum melting temperature is $T^* \sim 10^2\delta_m^6$ eV, the cold-melting density is $\rho^* \sim 10^8\delta_m^{12}$ g/cm^3, and the corresponding pressure is $P \sim 10^{16}Z^{10}A^{20/3}\delta_m^{20}$ Mbar. We emphasize once more the low reliability of these values, in view of their strong dependence on δ_m. Figure 5 shows a qualitative melting curve, the thick section of which corresponds to a classical crystal.

In connection with the mention made in the main text of cold melting of liquid helium, let us point out a specific feature of this case. The interaction of helium atoms is characterized by strong repulsion at short distances, like $1/r^n$ with $n > 2$ (overlap of electron shells). The binding energy is therefore of the order of $1/D^n \sim N^{n/3}$. The average oscillation frequency is determined by the quantity $|\partial^2U/\partial r^2|^{1/2} \sim 1/D^{1+n/2} \sim N^{1/3+n/6}$. The ratio of $\hbar\langle\omega\rangle$ to the binding energy is therefore of the order of $N^{(2-n)/6}$. At $n < 2$ we obtain the case considered in the text, namely, melting occurs when the pressure increases. At $n < 2$ we obtain

the opposite situation, which indeed corresponds to the diagram of state of helium.

The condition under which the Coulomb effects for nuclei become appreciable with the energy of the Gamow peak are determined by the relation $D \sim L^{eff}$, where $L^{eff} = (\tau T/Z^2e^2N)^{1/2}$ is the effective Debye radius. This gives the relation (see curve 2 of Fig. 6)

$$\rho^* \sim \frac{M^2}{e^2\hbar^2} T^{*2},$$

which has occurred already earlier for curve 4 of Fig. 3. The limit of the classical motion of the lattice nuclei under the same conditions is given by the relation $\tau T \sim \hbar\omega_D$ or

$$\rho^* \sim \left(\frac{M^4e}{\hbar^5}\right)^{2/3} T^{*4/3}$$

(see curve 3 of Fig. 6).

4. POSITRON AND NEUTRON FORMS OF MATTER

The production of electron-positron pairs in hot matter is described by the relations $\mu_+ + \mu_- = 0$ and $n_- - n_+ = n_0$, where n_0 is the initial electron concentration, and the indices (+) and (-) pertain to positrons and electrons, respectively, hence

$$n_\pm \sim \int d^3p n_{\pm p}, \quad P_+ \sim \int d^3p \varepsilon(p) n_{+p},$$

$$n_{\pm p} \equiv \left[\exp\frac{\varepsilon(p) \pm \mu}{T} + 1\right]^{-1}, \quad \mu = \mu_- = -\mu_+ \text{ and } \int d^3p (n_{-p} - n_{+p}) \sim n_0.$$

For $T \gg mc^2$ we have $n_+ \sim (T/\hbar c)^3$ and $P_+ \sim T^4/\hbar^3c^3$, and for $T < mc^2$

$$n_+ \sim \frac{(mT)^{3/2}}{\hbar^3} e^{-2mc^2/T}, \quad P_+ \sim T\frac{(mT)^{3/2}}{\hbar^3} e^{-mc^2/T}$$

(see curve 2 of Fig. 7).

Neutronization of cold matter begins when the electron concentration reaches the value given by

$$c((3\pi^2\hbar^3n)^{2/3} + m^2c^2)^{1/2} = \Delta Mc^2.$$

The expression for the threshold density is therefore

$$\rho \approx \frac{1Mc^3}{3\pi^2Z\hbar^3}[(\Delta M)^2 - m^2]^{3/2}.$$

When $\Delta M \gg m$ the threshold pressure is given by the formula $P \sim \hbar cn^{4/3} \sim c^5(\Delta M)^4/\hbar^3$. When $\Delta M \sim m$ it is necessary to use the equation of state of a relativistic degenerate electron gas (see[2]).

[1] L. D. Landau and E. M. Lifshitz, Statisticheskaya fizika (Statistical Physics), Nauka, 1964, Chaps. VII and XI.

[2] Ya. B. Zel'dovich and I. D. Novikov, Relyativistskaya astrofizika (Relativistic Astrophysics), Nauka, 1967, Sec. II.

[3] V. A. Ambartsumyan and G. S. Saakyan, Voprosy kosmogonii 9, 91 (1963). G. S. Saakyan, in: Problemy sovremennoĭ kosmogonii (Problems of Modern Cosmogony), Nauka, 1969, p. 240.

[4] D. A. Kirzhits, Polevye metody teorii mnogikh chastits (Field Methods of Many-body Theory), Gosatomizdat, 1963, Sec. 6.

[5] S. G. Brush, H. S. Sahlin, and E. Teller, J. Chem. Phys. 45, 2102 (1966).

[6] S. G. Brush, In: Progress of High Temperature Physics and Chemics, vol. 1, 1967.

[7] J. Linhart, Suppl. Nuovo Cimento 6, 913 (1968).

[8] P. W. Bridgman, The Physics of High Pressure, Bell, 1931; Recent Work in the Field of High Pressures, Revs. Mod. Phys. 18, 1 (1946).

[9] C. Swenson, High Pressure Physics (Russ. Transl.) IL, 1948.

[10] L. F. Vereshchagin, Vysokie davleniya v tekhnike budushchego (High Pressures in the Technology of the Future), AN SSSR, 1956; Rentgenostrukturnye issledovaniya veshchestva pri vycokikh davleniyakh (Magnetostructural Research on Matter at High Pressures), Supplement to[9].

[11] L. V. Al'tshuler, Usp. Fiz. Nauk 85, 197 (1965) [Sov. Phys.-Usp. 8, 52 (1965)]; L. V. Al'tshuler and A. A. Bakanova, ibid. 96, 193 (1968) [11, 678 (1969)].

[12] Ya. B. Zel'dovich and Yu. P. Raĭzer, Fizika udarnykh voln i vysokotemperaturnykh gidrodinamicheskikh yavlenii (Physics of Shock Wave and High Temperature Hydrodynamic Phenomena), Moscow, Fizmatgiz, 1963.

[13] S. B. Kormer, Usp. Fiz. Nauk 94, 641 (1968) [Sov. Phys.-Usp. 11, 229 (1968)].

[14] V. V. Evdokimova, ibid. 88, 93 (1966) [9, 54 (1966)].

[15] S. M. Stishov, ibid. 96, 467 (1968) [11, 816 (1969)].

[16] N. B. Brandt and N. I. Ginzburg, ibid. 85, 485 (1965) and 98, 95 (1969) [8, 202 (1965) and 12, 344 (1969)].

[17] V. N. Zharkov and V. A. Kalinin, Uravneniya sostoyaniya tverdykh tel pri vysokikh davleniyakh i temperaturakh (Equations of State of Solids at High Pressures and Temperatures), Nauka, 1968.

[18] A. I. Voropinov, G. M. Gandel'man, and V. T. Podval'nyĭ, Usp. Fiz. Nauk 100, 193 (1970) [Sov. Phys.-Usp. 13, 56 (1970)].

[19] R. Post, High Temperature Plasma and Controlled Thermonuclear Reactions (Russ. transl.) IL, 1961.

[20] D. A. Frank-Kamenetskiĭ, Plasma-chetvertoe sostoyanie veshchestva (Plasma, The Fourth State of Matter), Gosatomizdat, 1961.

[21] L. A. Artsimovich, Upravlyaemye termoyadernye reaktsii (Controlled Thermonuclear Reactions), Fizmatgiz, 1963. Elementarnaya fizika plazmy (Elementary Plasma Physics) 3-rd ed. Atomizdat, 1969.

[22] V. A. Magnitskii, Vnutrennee stroenie i fizika zemli (Internal Structure and Physics of the Earth), Nedra, 1965.

[23] L. H. Aller, Astrophysics, Ronald, 1954.

[24] E. Schatzman, White Dwarfs, Amsterdam, 1957.

[25] Proc. Sumpos. on Low-luminosity Stars, Virginia, USA, 1968.

[26] A. Hewish, Scientific American 219 (4), 25 (1969).

[27] V. L. Ginzburg, Pul'sary (Pulsars), Znanie, 1970; Usp. Fiz. Nauk 103, 393 (1971) [Sov. Phys.-Usp 14, 83 (1971)].

[28] D. Pines, Inside Neutron Stars, Preprint Nordita, August 1970.

[29] N. G. Basov and O. N. Krokhin, Zh. Eksp. Teor. Fiz. 46, 171 (1964) [Sov. Phys.-JETP 19, 123 (1964)].

[30] Ch. Maisonnier, Nuovo Cimento 62B, 332 (1966)].

[31] G. M. Gandel'man, V. M. Ermachenko, and Ya. B. Zel'dovich, Zh. Eksp. Teor. Fiz. 44, 386 (1963) [Sov. Phys.-JETP 17, 263 (1963)].

[32] D. A. Kirzhnits, Zh. Eksp. Teor. Fiz. 35, 1545 (1958) [Sov. Phys.-JETP 8, 1081 (1959)].

[33] N. N. Kalitkin, Zh. Eksp. Teor. Fiz. 38, 1534 (1960) [Sov. Phys.-JETP 11, 1106 (1960)]; Preprint, Appl. Math. Inst. USSR Acad. Sci., 1968.
[34] D. A. Kirzhnits, Zh. Eksp. Teor. Fiz. 38, 503 (1960) [Sov. Phys.-JETP 11, 365 (1960)].
[35] A. A. Abrikosov, Zh. Eksp. Teor. Fiz. 39, 1797 (1960) [Sov. Phys.-JETP 12, 1254 (1961)].
[36] E. Salpeter, Ap. J. 134, 669 (1961).
[37] L. Mestel and M. Ruderman, Month. Not. 136, 27 (1967).
[38] H. Van Horn, Phys. Lett. 28A, 706 (1969).
[39] H. Van Horn, Ap. J. 151, 227 (1968).
[40] W. Carr, Phys. Rev. 122, 1437 (1961).
[41] J. Dugdale and J. Frank, Phil. Trans. A257, 1 (1964); J. Dugdale, Physics of High Pressure and the Condensed Phases, Amsterdam, 1965.
[42] P. Nozieres and D. Pines, Phys. Rev. 111, 446 (1958).
[43] F. de Wette, Phys. Rev. 137A, 287 (1964).
[44] H. Van Horn, Thesis (Cornell University, CRSR 211, 1965).
[45] M. Ruderman, Nature 218, 1128 (1968).
[46] G. Baym, C. Pethick, D. Pines, and M. Ruderman, Nature 224, 872 (1969).
[47] V. L. Ginzburg and D. A. Kirzhnits, Zh. Eksp. Teor. Fiz. 47, 2006 (1964) [Sov. Phys.-JETP 20, 1346 (1965)]; V. L. Ginzburg, Usp. Fiz. Nauk 97, 601 (1969) [Sov. Phys.-Usp. 12, 241 (1969)].
[48] D. A. Kirzhnits, Izv. vuzov (Radiofizika) 13, 1847 (1970).
[49] E. Salpeter and H. Van Horn, Ap. J. 155, 183 (1970).
[50] D. A. Frank-Kamenetskiĭ, Fizicheskie protsessy vnutri zvezd (Physical Processes Inside Stars) Fizmatgiz, 1959.
[51] V. P. Kopyshev, Astron. zh. 8, 691 (1965).
[52] W. Wildhack, Phys. Rev. 57, 81 (1940).
[53] Ya. B. Zel'dovich, Zh. Eksp. Teor. Fiz. 33, 991 (1957) [Sov. Phys.-JETP 6, 760 (1958)].
[54] V. S. Imshennik and D. K. Nadezhin, Astron. zh. 42, 1154 (1965) [Sov. Astron. AJ 9, 896 (1966)].
[55] J. A. Wheeler, in: Gravitation and Relativity, Benjamin, 1964; J. A. Wheeler, B. Harrison, M. Vacano, and K. Thorne, Theory of Gravitation and Gravitational Collapse (Russ. transl.), Mir, 1967.
[56] A. G. W. Cameron, Neutron Stars, Lectures, Preprint (1969).
[57] V. A. Ambartsumyan and G. S. Saakyan, Astron. zh. 37, 193 (1960) [Sov. Astron.-AJ 4, 187 (1960)]; G. S. Saakyan and Yu. L. Vertanyan, Soobshch. Byurakansk obs. 33, 55 (1963).
[58] A. G. W. Cameron, Ap. J. 150, 884 (1959).
[59] W. Langer and L. Rosen, Astr. Space Sci. 6, 217 (1970).
[60] Voltaire, Micromégas, Romans, vol. 1, Paris, 1887.
[61] J. McDougall and E. Stoner, Phil. Trans. A237, 67 (1938).
[62] V. A. Volodin and D. A. Kirzhnits, ZhETF Pis. Red. 13, 450 (1971) [JETP Lett. 13, 320 (1971); D. A. Kirzhnits, Trudy Mezhdun. konf. po fizike tyazhelykh ionov (Proc. Internat Conf. on Heavy Ion Physics), Dubna, 1971.

Translated by J. G. Adashko